Chapter 12

Electronic Stability Program

Ground vehicles can be guided out of a straight path thanks to the control of their steerable wheels and to the overall yaw torque induced by the forces generated by the tires. In this context, the Electronic Stability Program (ESP) translates the steering wheel angle, conceived as a driver reference input, into a reference equilibrium trajectory, in the state space, and regulates the yaw torque to make the vehicle to follow it. The vehicle dynamics specialised for the study of the ESP problem is detailed in Section 12.1 whereas its modes are investigated in Section 12.1.1. The control problem that characterises the ESP is introduced in Section 12.2. The reference generator that translates the steering angle into a desired yaw rate and side-slip angle is presented in Section 12.3. Finally, the ESP tracking performances are evaluated in Section 12.4.

Contents

12.1 3DOF Vehicle Model

For the study of the horizontal dynamics of a four wheels vehicle we refer to the scheme of Figure 12.1. The vehicle is conceived as a point mass of mass and (yaw) inertia $m, \mathrm{J} > 0$. The geometry of the vehicle is defined by means

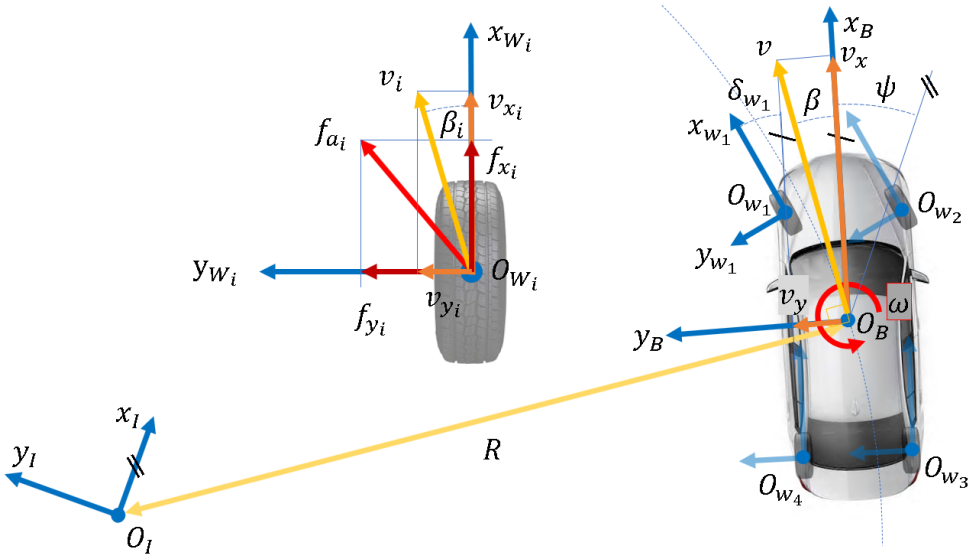

Figure 12.1: 3DOF (two translations and one rotation) model of a four wheels vehicle for the study of the horizontal dynamics.

of the vectors $\mathbf{r}_i := \texttt{col}(r_{x_i}, r_{y_i}) \in \mathbb{R}^2$ that describe the horizontal position of the i-th wheel centre, namely O_{W_i}, with respect to the local axes x_B-O_B-y_B. Each wheel generates a friction force, namely f_{a_i}, whose components are described in the local wheel frame x_{W_i}-O_{W_i}-y_{W_i}. The angle between the inertial x-axis and the body x-axis is denoted by ψ and represents the so called *yaw* angle whereas the angle between the inertial speed v and the local x_B axis is called *side-slip* angle and is denoted with β. Moreover, the angle the wheels are tilted with respect to the x_B-axis are denoted with δ_{W_i}. Finally, we conceive this system equipped with a gyroscope measuring the angular speed ω and a tachometer providing v.

The dynamics of the plant is given by

$$\begin{bmatrix} m\dot{v}_x \\ m\dot{v}_y \\ \mathrm{J}\dot{\omega} \end{bmatrix} = \begin{bmatrix} f_x + m\omega v_y - \frac{1}{2}\rho S v^2 C_D \\ f_y - m\omega v_x \\ \tau \end{bmatrix} \tag{12.1a}$$

where $f_x, f_y \in \mathbb{R}$ represent the longitudinal and lateral forces (in the frame x_B-O_B-y_B) and $\tau \in \mathbb{R}$ denotes the yaw torque. These three quantities are

induced by the tires and given by

$$
\begin{aligned}
f_x &= \sum_{i=1}^{4} \left(\cos \delta_{W_i} f_{x_i} - \sin \delta_{W_i} f_{y_i} \right) \\
f_y &= \sum_{i=1}^{4} \left(\sin \delta_{W_i} f_{x_i} + \cos \delta_{W_i} f_{y_i} \right) \\
\tau &= \sum_{i=1}^{4} \left(\sin \delta_{W_i} f_{y_i} - \cos \delta_{W_i} f_{x_i} \right) r_{y_i} + \left(\sin \delta_{W_i} f_{x_i} + \cos \delta_{W_i} f_{y_i} \right) r_{x_i}
\end{aligned}
\tag{12.1b}
$$

where $f_{x_i}, f_{y_i} \in \mathbb{R}$ denote the longitudinal and lateral force induced by the i-th tire (in the frame x_{W_i}-O_{W_i}-y_{W_i}). To reduce the complexity of the problem we assume that the rear wheels cannot be tilted, so that $\delta_{W_3} = \delta_{W_4} = 0$, whereas for the front wheels we assume as degree of freedom the value of the steering wheel $\delta_f \in \mathbb{R}$ and, given the kinematic chains $f_{1_\delta}, f_{2_\delta} : \mathbb{R} \mapsto \mathbb{R}$ that describe the steering system kinematics, we define $\delta_{W_1} = f_{1_\delta}(\delta_f)$ and $\delta_{W_2} = f_{2_\delta}(\delta_f)$. The forces f_{x_i} and f_{y_i} are, in turn, given by

$$
f_{x_i} = N_i \mu \left(\lambda_i, \boldsymbol{\Theta}_{\lambda_i} \right), \quad f_{y_i} = -N_i \mu \left(\beta_i, \boldsymbol{\Theta}_{\beta_i} \right) \tag{12.1c}
$$

with $N_i > 0$ denoting the vertical load and where $\lambda_i \in [-1, 1]$ and $\beta_i \in [-\pi/2, \pi/2]$ are the longitudinal slip ratio and the wheel side-slip angle respectively. The function $\mu(s)$ represents the friction coefficient model provided by (*Burckhardt*)

$$
\mu \left(s, \boldsymbol{\Theta}_s \right) = \Theta_{1_s} \left(1 - e^{-s\Theta_{2_s}} \right) - s\Theta_{3_s} \tag{12.1d}
$$

where $\boldsymbol{\Theta}_s := \texttt{col}(\Theta_{1_s}, \Theta_{2_s}, \Theta_{3_s})$ are parameters. The wheel side-slip angle is defined as

$$
\beta_i = \tan^{-1} \left(\frac{v_{y_i}}{v_{x_i}} \right) \tag{12.1e}
$$

where

$$
\begin{bmatrix} v_{x_i} \\ v_{y_i} \end{bmatrix} = \begin{bmatrix} \cos \delta_{W_i} & \sin \delta_{W_i} \\ -\sin \delta_{W_i} & \cos \delta_{W_i} \end{bmatrix} \left(\omega \begin{bmatrix} -r_{y_i} \\ r_{x_i} \end{bmatrix} + \begin{bmatrix} v_x \\ v_y \end{bmatrix} \right) \tag{12.1f}
$$

represent the longitudinal and lateral components of the speed of the wheel centre O_{W_i} (expressed in the frame x_{W_i}-O_{W_i}-y_{W_i}).

Infobox 12.1 *The model* (12.1) *considers the vertical tyre loads, N_i, as functions of the current speeds v_x and v_y,and yaw rate ω only. Instead, the real N_i are also functions of the accelerations $\dot{v}_x$ and $\dot{v}_y$ and yaw*

acceleration $\dot{\omega}$. Then, assuming for each $i = 1, \dots, 4$

$$N_i := \mathbf{H}_{i_1} \begin{bmatrix} \dot{v}_x \\ \dot{v}_y \\ \dot{\omega} \end{bmatrix} + H_{i_2}(v_x, v_y, \omega)$$

for some matrix $\mathbf{H}_{i_1}$ and function H_{i_2}, and substituting these expressions in (12.1a)*, one can collect all the time derivative terms to the left side to obtain a more general formulation.*

Therefore, we can assume that the vehicle is equipped with a sensor suite composed by a tachometer, providing a measurement of v_x, and a gyroscope measuring ω. These two sensors are affected by the noises $\nu_v \in \mathbb{R}$ and $\nu_\omega \in \mathbb{R}$ respectively.

The system (12.1) can be represented as a non linear system

$$\begin{aligned} \dot{\mathbf{x}} &= \mathbf{f}(\mathbf{x}, \mathbf{u}, \mathbf{d}) \\ y &= h(\mathbf{x}, \mathbf{u}, \mathbf{d}) + \nu \end{aligned} \tag{12.2}$$

in which $\mathbf{x} := \texttt{col}(v_y, \omega)$ represents the state, $\mathbf{u} := \texttt{col}(\delta_f, \lambda_1, \dots, \lambda_4)$ is the control input vector, $\mathbf{d} := \texttt{col}(v_x, \boldsymbol{\Theta}_{\lambda_1}, \boldsymbol{\Theta}_{\beta_1}, \dots, \boldsymbol{\Theta}_{\lambda_4}, \boldsymbol{\Theta}_{\beta_4})$ denotes the disturbance vector, $y := y_\omega$ collects the measurement and, finally, $\nu := \nu_\omega$ represents the noise affecting the sensor.

As linearisation trajectory we take a straight path travelled at constant speed $v_0 > 0$ while keeping a trivial side speed $v_y = 0$. We further assume that the linearisation disturbance is $\mathbf{d}_0 = \texttt{col}(v_0, \boldsymbol{\Theta}_{\lambda_1}, \boldsymbol{\Theta}_{\beta_1}, \dots, \boldsymbol{\Theta}_{\lambda_4}, \boldsymbol{\Theta}_{\beta_4})$. Then, from (12.1a) we obtain

$$\begin{bmatrix} f_{x_0} \\ f_{y_0} \\ \tau_0 \end{bmatrix} = \begin{bmatrix} \frac{1}{2}\rho S v_0^2 C_D \\ 0 \\ 0 \end{bmatrix}$$

Moreover, we assume a null steering angle $\delta_{f_0} = 0$ and for the rear wheels we consider a pure rolling working condition, *i.e.* we assume that $\lambda_3 = \lambda_4 = 0$ (front-wheel drive).

$$\begin{aligned} f_{x_0} &= \sum_{i=1}^{2} N_i \mu(\lambda_i, \boldsymbol{\Theta}_{\lambda_i}) \\ \tau_0 &= \sum_{i=1}^{2} -N_i \mu(\lambda_i, \boldsymbol{\Theta}_{\lambda_i}) r_{y_i} \end{aligned} \tag{12.3a}$$

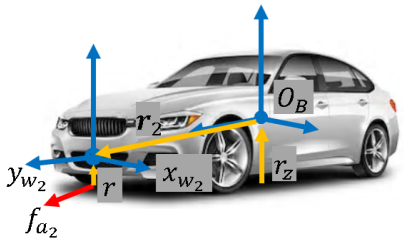

Figure 12.2: Vertical displacement of the reference frames

The (12.3) represents a set of non linear algebraic equations that can be solved to provide the equilibrium values of the unknowns λ_1 and λ_2 whose values depend on the loads N_i acting on the tires. To obtain these latter values we need to solve an hyper-static problem in which the vehicle is conceived at the equilibrium for the pitch and roll rotations and for the vertical translation. Assuming that O_B has an height of r_z from the ground (see Figure 12.2) we have that

$$\begin{bmatrix} N_1 \\ N_2 \\ N_3 \\ N_4 \end{bmatrix} = \begin{bmatrix} 1 & 1 & 1 & 1 \\ -r_{x_1} & -r_{x_2} & -r_{x_3} & -r_{x_4} \\ r_{y_1} & r_{y_2} & r_{y_3} & r_{y_4} \end{bmatrix}^{\dagger} \begin{bmatrix} mg \\ \frac{1}{2}\rho S v_0^2 C_D r_z - C_m \ell) \\ 0 \end{bmatrix}$$

where $()^{\dagger}$ denotes the right pseudo-inverse, $C_m \in \mathbb{R}$ represents the aerodynamic pitch momentum coefficient, and $\ell = r_{x_f} + r_{x_r}$ is the distance between the front and rear axles. Assuming $r_{x_1} = r_{x_2} = r_{x_f}$, $r_{x_3} = r_{x_4} = -r_{x_r}$, $r_{y_1} = r_{y_4} = r_y$ and $r_{y_2} = r_{y_3} = -r_y$, with $r_{x_f}, r_{x_r}, r_y > 0$, the four vertical forces are determined as

$$\begin{bmatrix} N_1 \\ N_2 \\ N_3 \\ N_4 \end{bmatrix} = \begin{bmatrix} r_{x_r} \\ r_{x_r} \\ r_{x_f} \\ r_{x_f} \end{bmatrix} \frac{mg}{2\left(r_{x_f} + r_{x_r}\right)} + \begin{bmatrix} -1 \\ -1 \\ 1 \\ 1 \end{bmatrix} \frac{C_D r_z - C_m (r_{x_f} + r_{x_r})}{2\left(r_{x_f} + r_{x_r}\right)} \frac{1}{2} \rho S v_0^2$$

where the first contribution is relative to the static loads and the second is relative to the pitch equilibrium.

Once identified the linearisation condition, *i.e.* the equilibrium triplet $(\mathbf{x}_0, \mathbf{u}_0, \mathbf{d_0})$, we defined the equilibrium output $y_0 = h(\mathbf{x}_0, \mathbf{u}_0, \mathbf{d_0})$ and the errors

$$\tilde{\mathbf{x}} = \mathbf{x} - \mathbf{x}_0, \quad \tilde{\mathbf{d}} = \mathbf{d} - \mathbf{d}_0, \quad \tilde{y} = y - y_0$$

whereas for the control input the error is specialised as

$$\tilde{\mathbf{u}} = \mathtt{col}(\tilde{u}_\delta, \tilde{\mathbf{u}}_\lambda) := \mathbf{u} - \mathbf{u}_0$$

in which $\tilde{u}_\delta := \delta_f - \delta_{f_0}$ and $\tilde{\mathbf{u}}_\lambda = \texttt{col}(\tilde{\lambda}_1, \dots, \tilde{\lambda}_4) := \texttt{col}(\lambda_1, \dots, \lambda_4) - \texttt{col}(\lambda_{1_0}, \dots, \lambda_{4_0})$. So, we linearise the system (12.2) around the equilibrium to obtain

$$\begin{aligned} \dot{\tilde{\mathbf{x}}} &= \mathbf{A}\tilde{\mathbf{x}} + \mathbf{B}_{1_\delta}\tilde{u}_\delta + \mathbf{B}_{1_\lambda}\tilde{\mathbf{u}}_\lambda + \mathbf{B}_2\tilde{\mathbf{d}} \\ \tilde{y} &= \mathbf{C}_1\tilde{\mathbf{x}} + \nu \end{aligned} \tag{12.4}$$

with

$$\mathbf{A} = \begin{bmatrix} -\dfrac{C_{\beta_f} + C_{\beta_r}}{mv_0} & -\dfrac{C_{\beta_f} r_{x_f} - C_{\beta_r} r_{x_r}}{mv_0} - v_0 \\ -\dfrac{C_{\beta_f} r_{x_f} - C_{\beta_r} r_{x_r}}{\mathrm{J}v_0} & -\dfrac{C_{\beta_f} r_{x_f}^2 + C_{\beta_r} r_{x_r}^2}{\mathrm{J}v_0} \end{bmatrix}$$

$$\mathbf{B}_{1_\delta} = \begin{bmatrix} \dfrac{C_{\beta_f}}{m} \\ \dfrac{C_{\beta_f} r_{x_f}}{\mathrm{J}} \end{bmatrix}, \quad \mathbf{B}_{1_\lambda} = \frac{1}{\mathrm{J}} \begin{bmatrix} 0 & \dots & 0 \\ \dfrac{\partial \tau}{\partial \lambda_1} & \dots & \dfrac{\partial \tau}{\partial \lambda_4} \end{bmatrix}, \quad \mathbf{C}_1 = \begin{bmatrix} 0 & 1 \end{bmatrix}$$

in which we have assumed $\left.\dfrac{\partial f_{1_\delta}}{\partial \delta_f}\right|_0 = \left.\dfrac{\partial f_{2_\delta}}{\partial \delta_f}\right|_0 = 1$ and where C_{β_f} and C_{β_r}, called *cornering stiffness* of the front and rear axle respectively, beside $\partial\tau/\partial\lambda_i$ are defined as

$$\begin{aligned} C_{\beta_f} &:= \sum_{i=1}^{2} N_{i_0} \frac{\partial}{\partial \beta_i} \mu\left(\beta_i, \mathbf{\Theta}_{\beta_i}\right) \\ C_{\beta_r} &:= \sum_{i=3}^{4} N_{i_0} \frac{\partial}{\partial \beta_i} \mu\left(\beta_i, \mathbf{\Theta}_{\beta_i}\right) \\ \frac{\partial \tau}{\partial \lambda_i} &= -N_i \frac{\partial \mu\left(\lambda_{i_0}, \mathbf{\Theta}_{\lambda_{i_0}}\right)}{\partial \lambda_i} r_{y_i} \end{aligned}$$

12.1.1 Modal Analysis

The eigenvalues of $\mathbf{A}$ are found as the roots of

$$\begin{aligned} \det(\mathbf{A} - s\mathbf{I}) = \det\left(\begin{bmatrix} -\dfrac{C_{\beta_f} + C_{\beta_r}}{mv_0} - s & -\dfrac{C_{\beta_f} r_{x_f} - C_{\beta_r} r_{x_r}}{mv_0} - v_0 \\ -\dfrac{C_{\beta_f} r_{x_f} - C_{\beta_r} r_{x_r}}{\mathrm{J}v_0} & -\dfrac{C_{\beta_f} r_{x_f}^2 + C_{\beta_r} r_{x_r}^2}{\mathrm{J}v_0} - s \end{bmatrix}\right) = \\ = s^2 + s\left(\frac{C_{\beta_f} + C_{\beta_r}}{mv_0} + \frac{C_{\beta_f} r_{x_f}^2 + C_{\beta_r} r_{x_r}^2}{\mathrm{J}v_0}\right) + \\ \frac{C_{\beta_f} C_{\beta_r} (r_{x_f} + r_{x_r})^2}{m\mathrm{J}v_0^2}\left(1 + \frac{\eta v_0^2}{g\left(r_{x_f} + r_{x_r}\right)}\right) = 0 \end{aligned}$$

where

$$\eta := -mg\frac{C_{\beta_f}r_{x_f} - C_{\beta_r}r_{x_r}}{C_{\beta_f}C_{\beta_r}\left(r_{x_f} + r_{x_r}\right)}$$

is called *understeering gradient*. Then, the system has negative real part eigenvalues if

$$(a) \quad \frac{C_{\beta_f} + C_{\beta_r}}{mv_0} + \frac{C_{\beta_f}r_{x_f}^2 + C_{\beta_r}r_{x_r}^2}{\mathrm{J}v_0} > 0$$

$$(b) \qquad 1 + \frac{\eta v_0^2}{g\left(r_{x_f} + r_{x_r}\right)} > 0$$

The condition (a) is always verified whereas the condition (b) is verified for

- $\eta \geq 0$ for any $v_0 > 0$;
- $\eta < 0$ for $v_0 < v_{\mathrm{cr}}$ with

$$v_{\mathrm{cr}} := \sqrt{-\frac{g}{\eta}\left(r_{x_f} + r_{x_r}\right)}$$

  denoting the so called *critical speed*.

Moreover, for $\eta < 0$, at $v_0 = v_{\mathrm{cr}}$ the eigenvalues are

$$s_1 = 0 \qquad s_2 = -\frac{C_{\beta_f} + C_{\beta_r}}{mv_0} - \frac{C_{\beta_f}r_{x_f}^2 + C_{\beta_r}r_{x_r}^2}{\mathrm{J}v_0}$$

whereas for $\eta > 0$ the eigenvalues are purely real negative (null imaginary part) for $v_0 \leq v_r$ where

$$v_r := \frac{1}{2}\sqrt{\left[\left(\frac{C_{\beta_f} + C_{\beta_r}}{m} + \frac{C_{\beta_f}r_{x_f}^2 + C_{\beta_r}r_{x_r}^2}{\mathrm{J}}\right)^2 - 4\frac{C_{\beta_f}C_{\beta_r}(r_{x_f} + r_{x_r})^2}{m\mathrm{J}}\right]} \times \sqrt{\frac{mg\mathrm{J}}{\eta C_{\beta_f}C_{\beta_r}\left(r_{x_f} + r_{x_r}\right)}}.$$

Finally, for $\eta = 0$ the eigenvalues are always purely real negative (null imaginary part). Figure 12.3 graphically depicts the eigenvalues of $\mathbf{A}$ as function of the vehicle speed v_0. These diagrams, jointly with the plots of Figures 12.4 and 12.5, make clear the physical phenomenon.

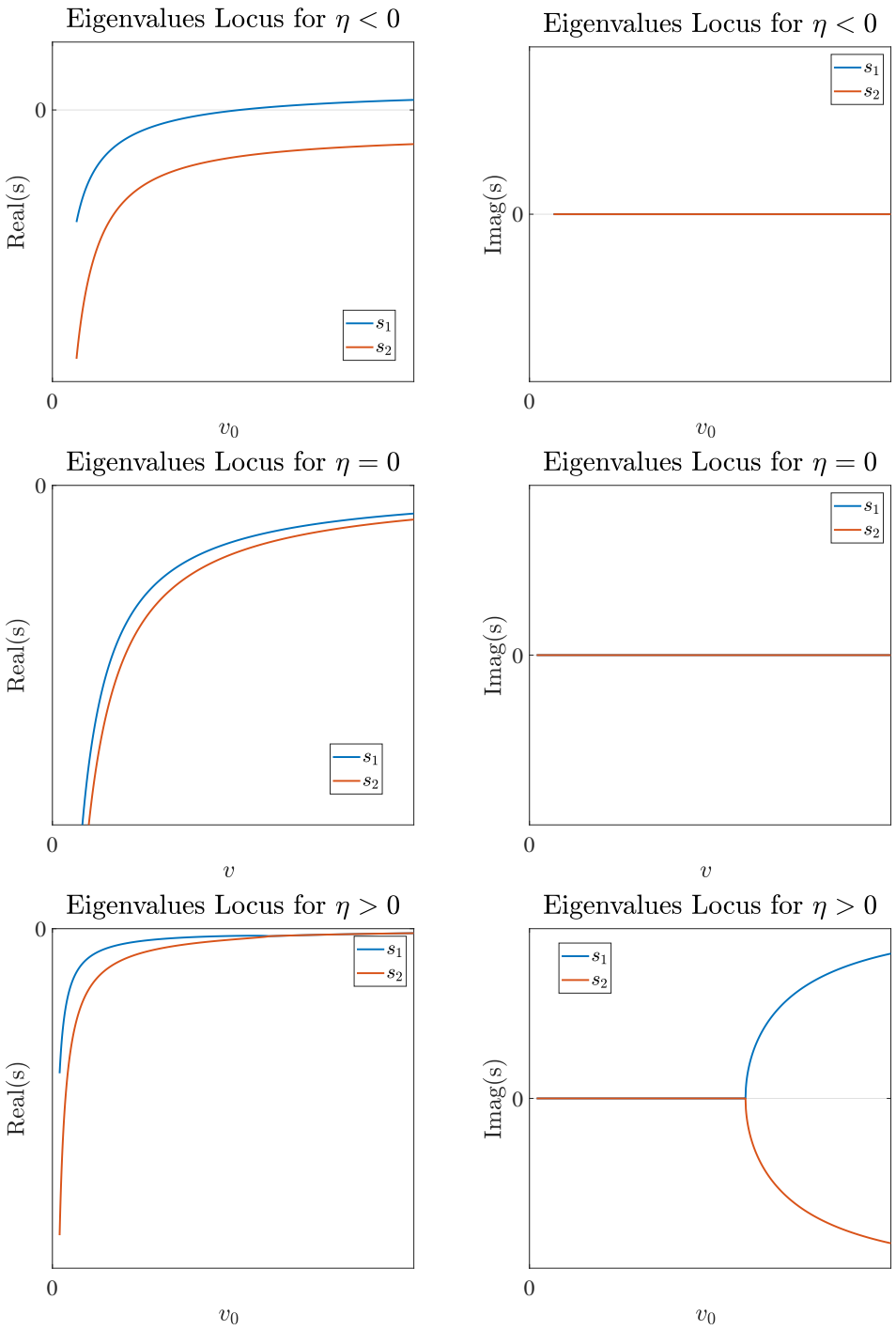

Figure 12.3: Locus of the eigenvalus of $\mathbf{A}$ for η negative, null and positive as function of v_0.

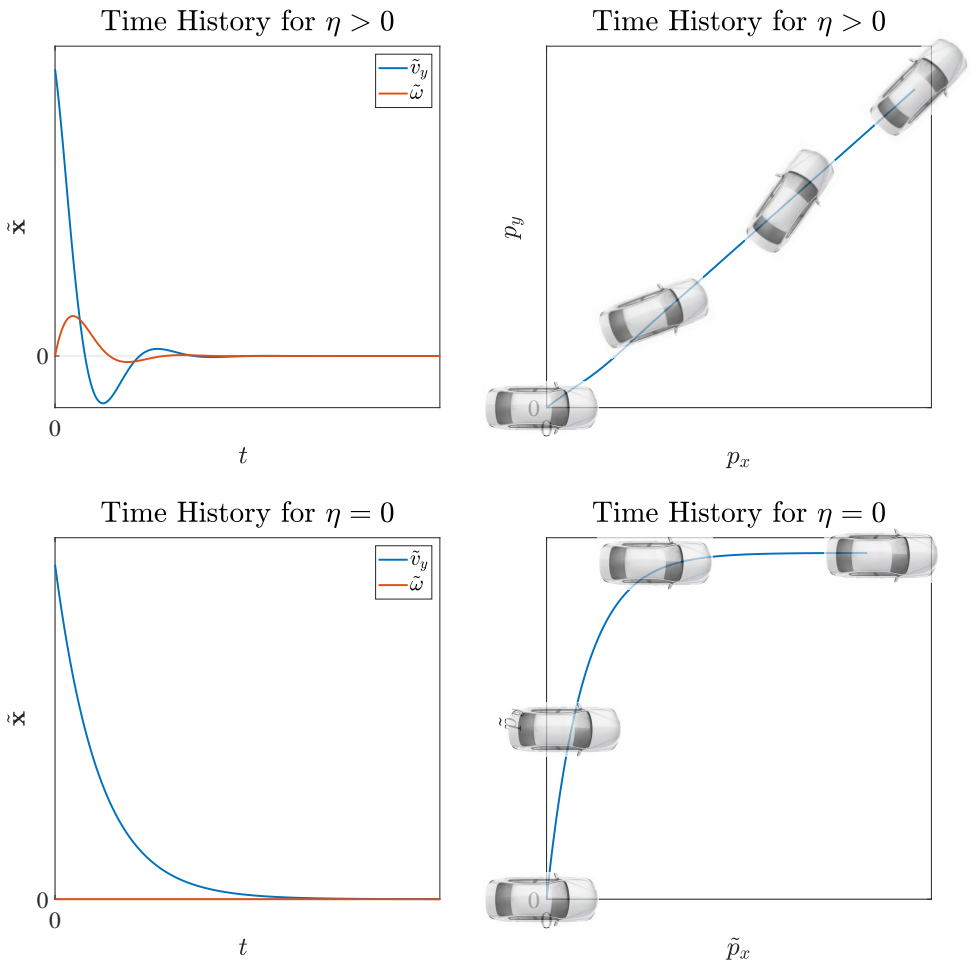

Figure 12.4: Behaviour of vehicle characterised by $\eta \geq 0$. When $\eta = 0$ the dynamics of $\tilde{v}_y$ and $\tilde{\omega}$ are decoupled and, for this reason, the vehicle skids laterally until the friction force reduces $\tilde{v}_y$ to zero. On the other hand, the vehicle with $\eta > 0$ are naturally stable assessed by a self-aligning behaviour that reduces $\tilde{v}_y$ to zero.

12.2 Control Problem Setup

The goal of the ESP is twofold: stabilise the system (or increase the stability if already stable) and track a reference state, namely $\tilde{\mathbf{x}}^\star$, suitably associated to the steering wheel driver input $\tilde{u}_\delta$. To this end, we consider $\tilde{\mathbf{u}}_\delta$ as well as its associated reference $\tilde{\mathbf{x}}^\star$ as constant. Again, we observe that all the inputs in $\tilde{\mathbf{u}}_\lambda$ are redundant so, to simplify the design problem we define an

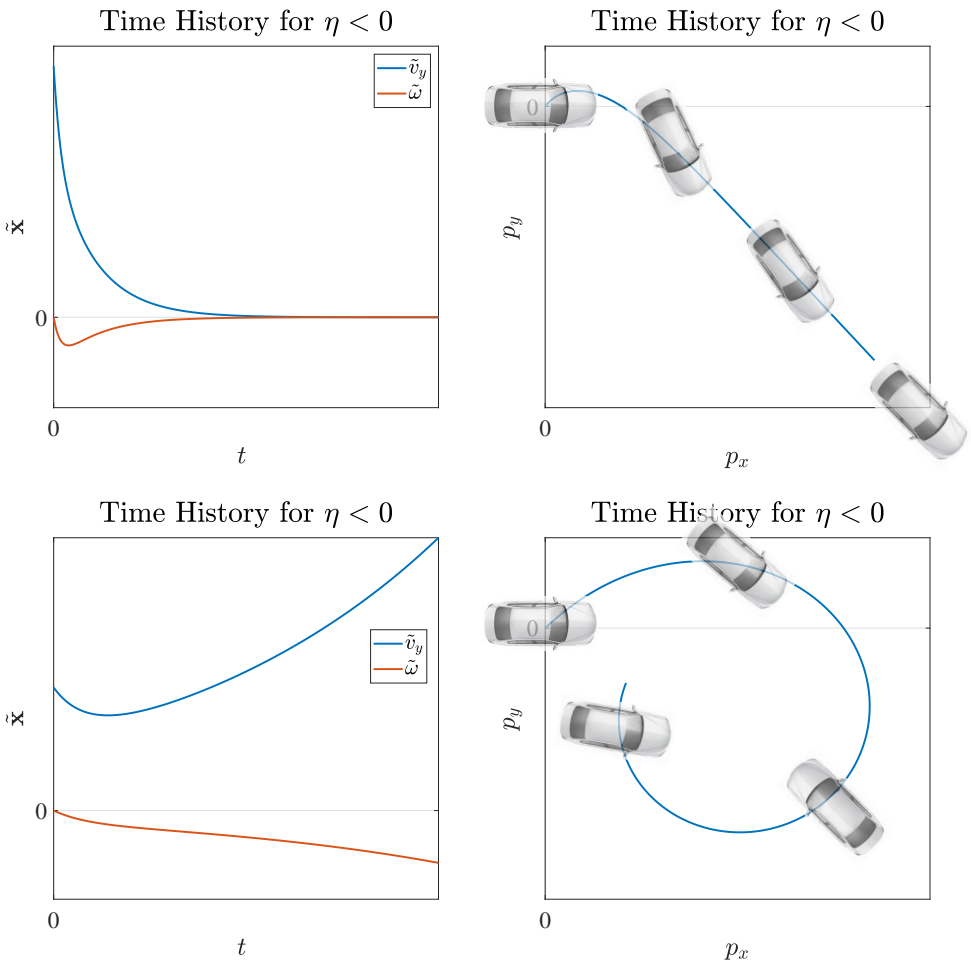

Figure 12.5: Behaviour of vehicle characterised by $\eta < 0$. The top pictures depict the dynamics of a vehicle travelling at $v_0 < v_{\text{cr}}$: in this case the trajectory evolves in a direction which is opposite with respect to that of the initial conditions but, thanks to the low speed, the self-alignment motion is still dominant. At the opposite, the bottom pictures describe the behaviour of a vehicle running at $v > v_{\text{cr}}$: the asymptotic path becomes non linear and the lateral and rotational speeds $\tilde{v}_y$ and $\tilde{\omega}$ are not bounded. The result is a loop with an increasing side-slip angle.

equivalent control, namely $\tilde{u}_{\text{eq}} \in \mathbb{R}$, such that

$$\mathbf{B}_{\text{eq}} \tilde{u}_{\text{eq}} = \mathbf{B}_{1_\lambda} \tilde{\mathbf{u}}_\lambda.$$

with $\mathbf{B}_{\text{eq}} = \texttt{col}(0, \text{J}^{-1})$. We now define the tracking error $\mathbf{e}_t = \mathbf{C}_e (\tilde{\mathbf{x}} - \tilde{\mathbf{x}}^\star)$ where $\mathbf{C}_e$ is a vector with only one row because, in agreement to what stated

in Section 4.5.3, this corresponds to the number of control input available. So, we consider for sake of simplicity $\tilde{\mathbf{d}} = \mathbf{0}$ and the state fully available so that we focus on a control system based on the state feedback (the estimation of the non linear state is described in Chapter 16).

Thus, for the stabilisation of the linear plant (12.4), we take the controller (4.38) in which the matrix $\mathbf{K}_R$ is defined by solving the stationary optimal control problem whose ingredients are

$$\begin{aligned}\begin{bmatrix} \dot{\tilde{\mathbf{x}}} \\ \dot{\boldsymbol{\eta}} \end{bmatrix} &= \begin{bmatrix} \mathbf{A} & \mathbf{0} \\ \mathbf{C}_e & \mathbf{0} \end{bmatrix} \begin{bmatrix} \tilde{\mathbf{x}} \\ \boldsymbol{\eta} \end{bmatrix} + \begin{bmatrix} \mathbf{B}_{\text{eq}} \\ \mathbf{0} \end{bmatrix} \tilde{u}_{\text{eq}} \\ \tilde{\mathbf{e}} &= \texttt{col}(\tilde{\mathbf{x}}, \boldsymbol{\eta}) \\ J &= \int_{t_0}^{\infty} \tilde{\mathbf{e}}^\top \mathbf{Q}_p \tilde{\mathbf{e}}^\top + R_p \tilde{u}_{\text{eq}}^2 \, dt\end{aligned}$$

The couple $(\mathbf{A}, \mathbf{B}_{\text{eq}})$ is fully reachable for any value of η implying the existence of a dynamic state feedback stabiliser of the form (4.35) in which the control $\tilde{\mathbf{u}}_\lambda$ is obtained as

$$\tilde{\mathbf{u}}_\lambda = \mathbf{B}_{1_\lambda}^\dagger \mathbf{B}_{\text{eq}} \tilde{u}_{\text{eq}}.$$

12.3 Reference Generator

The aim of the reference generator is that of providing to the stabiliser the reference $\tilde{\mathbf{x}}^\star$. To this end, we elaborate the pilot input δ_f by taking as a reference plant a vehicle with the same mass m and inertia J, the same geometry r_{x_f}, r_{x_r} but characterised by a positive understeering gradient. Thus, given $C_{\beta_f}^\star$, $C_{\beta_r}^\star$ such that $\eta^\star > 0$, for any δ_f we define the reference $\tilde{\mathbf{x}}^\star$ as

$$\begin{bmatrix} \tilde{v}_y^\star \\ \tilde{\omega}^\star \end{bmatrix} = \begin{bmatrix} \dfrac{C_{\beta_f}^\star + C_{\beta_r}^\star}{m v_0} & \dfrac{C_{\beta_f}^\star r_{x_f} - C_{\beta_r}^\star r_{x_r}}{m v_0} + v_0 \\ \dfrac{C_{\beta_f}^\star r_{x_f} - C_{\beta_r}^\star r_{x_r}}{\mathrm{J} v_0} & \dfrac{C_{\beta_f}^\star r_{x_f}^2 + C_{\beta_r}^\star r_{x_r}^2}{\mathrm{J} v_0} \end{bmatrix}^{-1} \begin{bmatrix} \dfrac{C_{\beta_f}^\star}{m} \\ \dfrac{C_{\beta_f}^\star r_{x_f}}{\mathrm{J}}. \end{bmatrix} \delta_f$$

Figures 12.6-12.7 depict the partial derivatives $\partial \tilde{v}_y^\star / \partial \delta_f$ and $\partial \tilde{\omega}^\star / \partial \delta_f$ as function of the linearisation speed v_0. These plots represent the sensitivity of the references $\tilde{v}_y^\star$, $\tilde{\omega}^\star$ with respect to the drive input and, to make clear why we chose a reference plant characterised by $\eta^\star > 0$, figure 12.6-12.7 also show these sensitivity functions for $\eta^\star \leq 0$.

More in details, the partial derivatives $\partial\tilde{v}_y^\star/\partial\delta_f$ and $\partial\tilde{\omega}^\star/\partial\delta_f$ are given by

$$\frac{\partial\tilde{v}_y^\star}{\partial\delta_f} = \frac{v_0\left(C_{\beta_f}^\star C_{\beta_r}^\star r_{x_r}\left(r_{x_r}+r_{x_f}\right) - mv_0^2 C_{\beta_f}^\star r_{x_f}\right)}{C_{\beta_f}^\star C_{\beta_r}^\star (r_{x_f}+r_{x_r})^2\left(1+\dfrac{\eta^\star v_0^2}{g\left(r_{x_f}+r_{x_r}\right)}\right)}$$

$$\frac{\partial\tilde{\omega}^\star}{\partial\delta_f} = \frac{v_0}{(r_{x_f}+r_{x_r})\left(1+\dfrac{\eta^\star v_0^2}{g\left(r_{x_f}+r_{x_r}\right)}\right)}$$

The lateral speed sensitivity $\partial\tilde{v}_y^\star/\partial\delta_f$ for $\eta^\star \geq 0$ is a continuous function with initial and asymptotic slopes opposite in sing that lead to a change of sign. Then, there exists a linearisation speed, namely $\bar{v}_0 > 0$, such that for all $0 < v_0 < \bar{v_0}$ the $\partial\tilde{v}_y^\star/\partial\delta_f$ is positive. Therefore, for $\eta^\star \geq 0$ and for $0 < v_0 < \bar{v_0}$ any positive increment of the steering wheel angle δ_f leads to a positive variation of the reference lateral speed $\tilde{v}_y^\star$. In practice, in these conditions, the reference lateral speed is positive and the vehicle will be induced to have a positive side-slip angle β (vehicle nose out of the tangent to the local turn trajectory). At the opposite, for $v_0 > \bar{v}_0$ the sensitivity $\partial\tilde{v}_y^\star/\partial\delta_f$ becomes negative inducing to a negative reference lateral speed $\tilde{v}_y^\star$ and, consequently to a negative side-slip angle β (vehicle nose inside the tangent to the local turn trajectory). Moreover, for $\eta^\star < 0$ the sensitivity $\partial\tilde{v}_y^\star/\partial\delta_f$ is undefined at the critical speed v_{cr} implying that any small variation of δ_f leads to a infinite variation of $\tilde{v}_y^\star$. Finally, the speed $\bar{v}_0$ is defined as

$$\bar{v}_0 = \sqrt{\frac{C_{\beta_r} r_{x_r}\left(r_{x_r}+r_{x_f}\right)}{m r_{x_f}}}.$$

The yaw rate sensitivity $\partial\tilde{\omega}^\star/\partial\delta_f$ is always positive and continuous for $\eta^\star \geq 0$ whereas for $\eta^\star < 0$ it becomes discontinuous at $v = v_{\text{cr}}$. The yaw rate sensitivity increases linearly for $\eta^\star = 0$ implying that, as the speed v_0 increases, the same variation δ_f leads to higher reference values of $\tilde{\omega}^\star$. Instead, for the case of $\eta^\star > 0$ the maximum yaw rate sensitivity is reached at $v = v_{\text{cr}}$. So, for $\eta^\star < 0$, positive steering wheel rotations leads to positive $\tilde{\omega}^\star$ for $v < v_{\text{cr}}$ and negative $\tilde{\omega}^\star$ for $v > v_{\text{cr}}$ whereas it is not defined (and not finite) at $v = v_{\text{cr}}$.

12.4 ESP evaluation

The ESP control is evaluated in two different conditions in which a vehicle is induced to be oversteered ($\eta < 0$) by introducing a positive road pitch

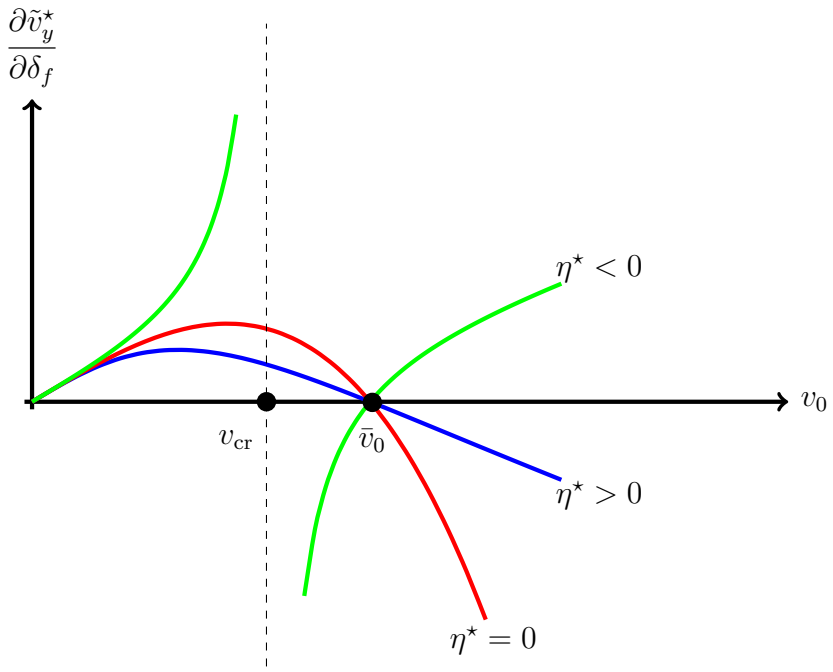

Figure 12.6: Lateral speed sensitivity $\frac{\partial \tilde{v}_y^\star}{\partial \delta_f}$ versus the speed v_0.

angle (nose down) that increases the load of the front wheels. In both the scenarios the vehicle starts travelling at a constant speed and, after 5 seconds, the simulated pilot rotates the steering wheel. In the first scenario (Figure 12.8) the vehicle is travelling at high speed $v_0 > v_{\rm cr}$ and the pilot steers the car with a one-period sinusoidal input (maximum amplitude of 5 degrees and period of 2 seconds). In the second scenario (Figure 12.9) the vehicle is travelling at low speed $v_0 < v_{\rm cr}$ and the pilot steers the wheels of a constant quantity (5 degrees). The first simulation is intended to show how the ESP can improve the stability of the plant whereas, in the second scenario the turning performance are under the spotlight. The control problem is solved by assuming $\mathbf{C}_e = [0\ 1]$ and by implementing the following listing.

```
%% Control Prolem Setup
% state penalization
Qx = inv(diag([(2)^2 (20/180*pi)^2]));
Qeta = 0.1*Ce*Qx*Ce.';
Qp = 1/3*blkdiag(Qeta,Qx);
% input penalization
Req = inv((ryf*2500)^2); % maximum force * side arm
% Controller design
Klqr = lqr(Ac,Bc,Qp,Req);
KR = -Klqr(2:3);
```

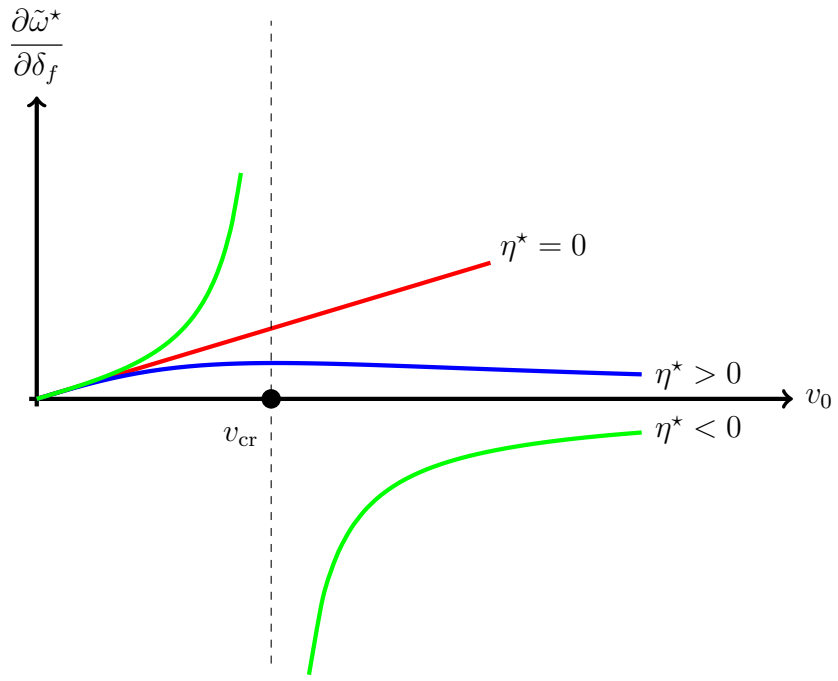

Figure 12.7: Yaw sensitivity $\dfrac{\partial\tilde{\omega}^\star}{\partial\delta_f}$ versus the speed v_0.

```
11 | Hs = -Klqr(1);
```

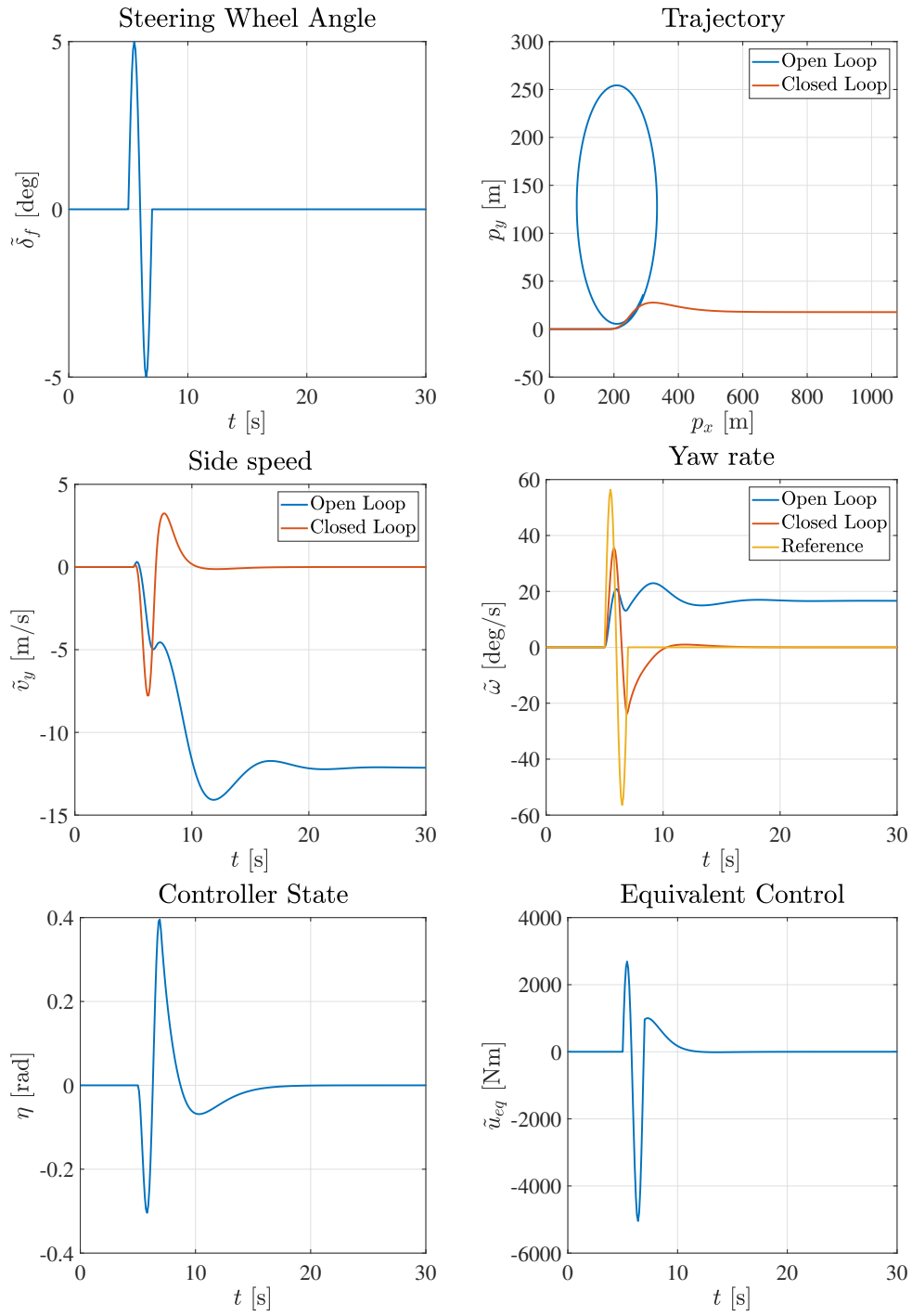

Figure 12.8: First Scenario: the vehicle is travelling at 130 km/h and the driver steers the wheels of 5 degrees in a sinusoidal way. As depicted in the top right figure, the open loop trajectory diverges from the straight path. The effect of the ESP in this scenario is that of restoring the stability, making the car to behave like an understeered vehicle ($\eta > 0$).

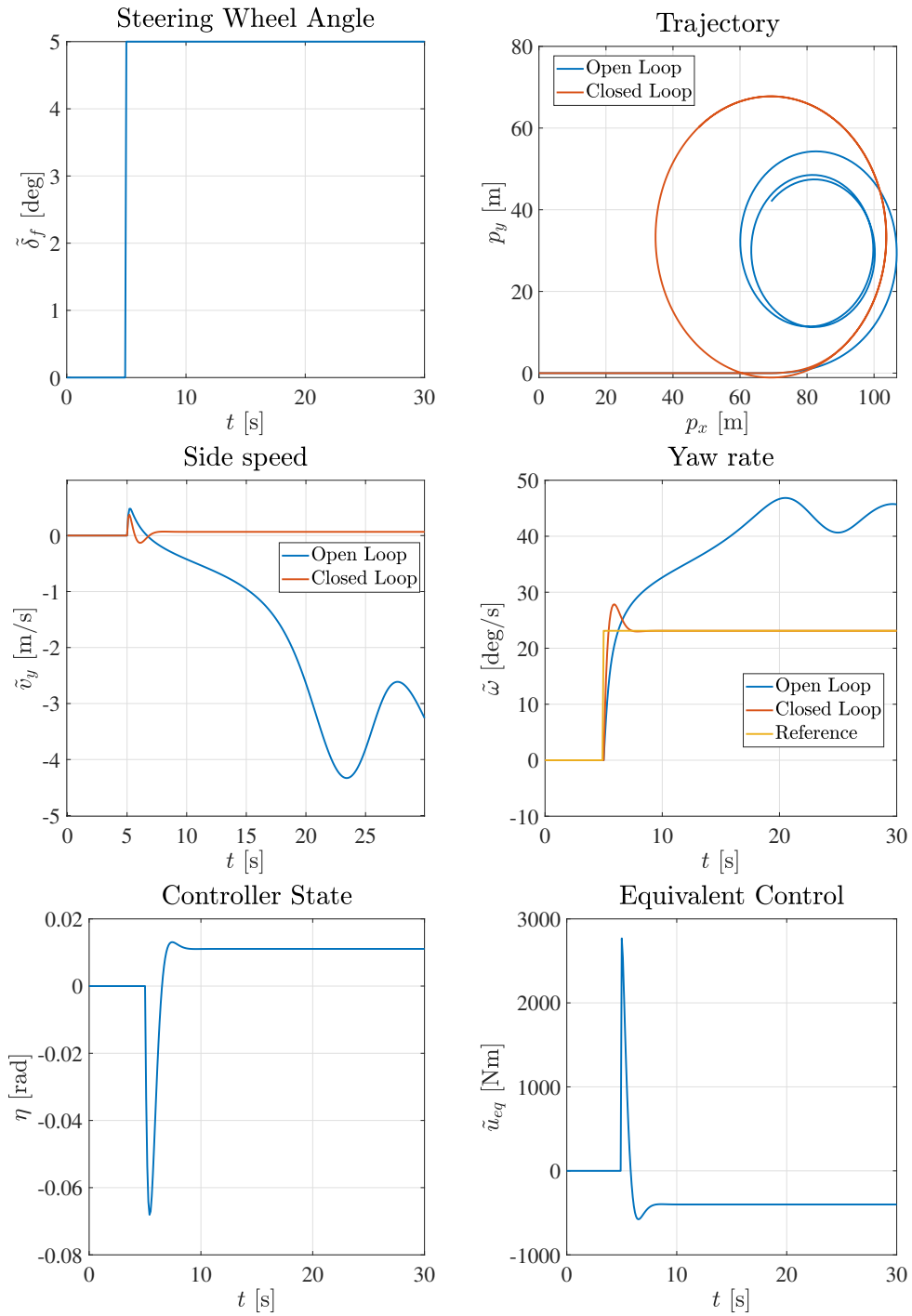

Figure 12.9: Second Scenario: the vehicle is travelling at 50 km/h and the driver steers the wheels of 5 degrees (left turn). As depicted in the top right figure, the open loop trajectory evolves on a circular path with a smaller radius due to the oversteering nature ($\eta < 0$) of the plant. The effect of the ESP in this scenario is that of restoring the desired curvature by tracking the reference yaw rate. As expected, the controller internal state η reaches an asymptotic value to compensate for the extra torque induced by the pilot through the steering wheel.

Bibliography

[Chen et al., 2016] Chen, W., Xiao, H., Wang, Q., Zhao, L., and Zhu, M. (2016). *Integrated vehicle dynamics and control*. John Wiley & Sons.

[Isermann, 2021] Isermann, R. (2021). *Automotive Control: Modeling and Control of Vehicles*. Springer-Verlag Berlin Heidelberg.

[Rajamani, 2012] Rajamani, R. (2012). *Vehicle Dynamics and Control*. Springer US.

[Ulsoy et al., 2012] Ulsoy, A. G., Peng, H., and Çakmakci, M. (2012). *Automotive control systems*. Cambridge University Press.